TECHNIQUE

Visualising and quantifying microvascular structure and function in patients with heart failure using optical coherence tomography

David F. G. Sciarrone[1], Robert A. McLaughlin[2,3,4] , Raden Argarini[1,5] , Minh-Son To[6,7],
Louise H. Naylor[1], Lucy M. Bolam[1], Howard H. Carter[1] and Daniel J. Green[1]

[1]*Cardiovascular Research Group, School of Human Sciences (Exercise and Sport Science), University of Western Australia, Perth, Australia*
[2]*Australian Research Council Centre of Excellence for Nanoscale Biophotonics, School of Biomedicine, Faculty of Health and Medical Sciences, University of Adelaide, Adelaide, Australia*
[3]*Institute for Photonics and Advanced Sensing, University of Adelaide, Adelaide, Australia*
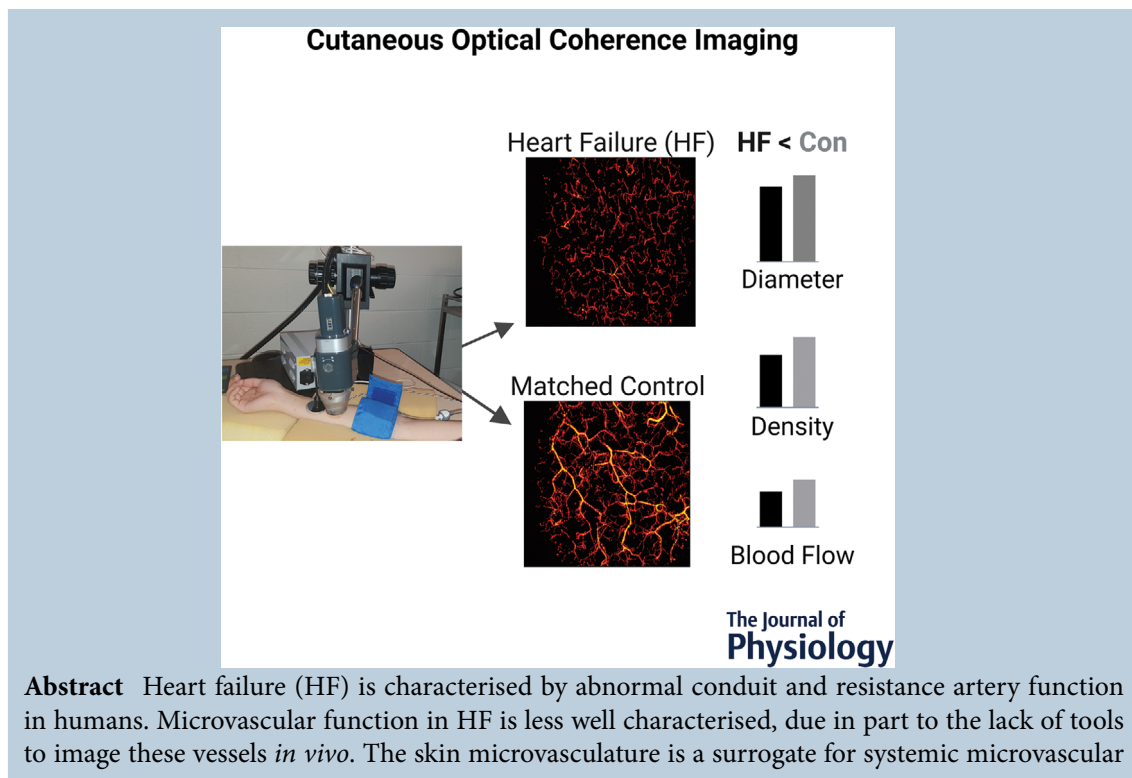[4]*School of Engineering, University of Western Australia, Perth, Australia*
[5]*Department of Medical Physiology and Biochemistry, Faculty of Medicine, Airlangga University, Surabaya, Indonesia*
[6]*Flinders Health and Medical Research Institute, Flinders University, Bedford Park, Australia*
[7]*Department of Neurosurgery, Flinders Medical Centre, Bedford Park, Australia*

Handling Editors: Harold Schultz & Philip Ainslie

The peer review history is available in the Supporting Information section of this article (https://doi.org/10.1113/JP282940#support-information-section).

The Journal of Physiology

Cutaneous Optical Coherence Imaging

Heart Failure (HF) **HF < Con**

Matched Control

Diameter

Density

Blood Flow

The Journal of **Physiology**

Abstract Heart failure (HF) is characterised by abnormal conduit and resistance artery function in humans. Microvascular function in HF is less well characterised, due in part to the lack of tools to image these vessels *in vivo*. The skin microvasculature is a surrogate for systemic microvascular

David F. G. Sciarrone and Robert A. McLaughlin shared first authorship.

function and health and plays a key role in thermoregulation, which is dysfunctional in HF. We deployed a novel optical coherence tomography (OCT) technique to visualise and quantify microvascular structure and function in 10 subjects with HF and 10 age- and sex-matched controls. OCT images were obtained from the ventral aspect of the forearm, at baseline (33°C) and after 30 min of localised skin heating. At rest, OCT-derived microvascular density ($20.3 \pm 8.7\%$, $P = 0.004$), diameter ($35.1 \pm 6.0 \mu$m, $P = 0.006$) and blood flow (82.9 ± 41.1 pl/s, $P = 0.021$) were significantly lower in HF than CON ($27.2 \pm 8.0\%$, $40.4 \pm 5.8 \mu$m, 110.8 ± 41.9 pl/s), whilst blood speed was not significantly lower ($74.3 \pm 11.0 \mu$m/s *vs.* $81.3 \pm 9.9 \mu$m/s, $P = 0.069$). After local heating, the OCT-based density, diameter, blood speed and blood flow of HF patients were similar (all $P > 0.05$) to CON. Although abnormalities exist at rest which may reflect microvascular disease status, patients with HF retain the capacity to dilate cutaneous microvessels in response to localised heat stress. This is a novel *in vivo* human observation of microvascular dysfunction in HF, illustrating the feasibility of OCT to directly visualise and quantify microvascular responses to physiological stimuli *in vivo*.

Corresponding author D. J. Green: Cardiovascular Research Group, School of Human Sciences (Exercise and Sports Science) M408, The University of Western Australia, 35 Stirling Highway, Nedlands 6009, Perth, Australia. Email: danny.green@uwa.edu.au

Abstract figure legend We have developed a powerful new, non-invasive optical coherence tomography imaging-based approach to study microvascular structure and function *in vivo*. This paper applies the technique to explore microvascular dysfunction in patients with heart failure (HF) *versus* matched controls (Con).

Key points

- Microvessels in the skin are critical to human thermoregulation, which is compromised in participants with heart failure (HF).
- We have developed a powerful new non-invasive optical coherence tomography (OCT)-based approach for the study of microvascular structure and function *in vivo*.
- Our approach enabled us to observe and quantify abnormal resting microvascular function in participants with HF.
- Patients with HF were able to dilate skin microvessels in response to local heat stress, arguing against an underlying structural abnormality. This suggests that microvascular functional regulation is the primary abnormality in HF.
- OCT can be used to directly visualise and quantify microvascular responses to physiological stimuli *in vivo*.

David F. G. Sciarrone is a medical student in the School of Medicine at The University of Western Australia (UWA). He completed his undergraduate degree in Biomedical Engineering, also at UWA, with an Honours thesis (First Class) about the deep learning-based quantification of microvessels in heart failure using optical coherence tomography. This current publication is an extension of this thesis, which was supervised by Senior Author Winthrop Professor Daniel J. Green and Professor Robert A. McLaughlin. He is interested in chronic cardiovascular disease research, the integration of deep learning into standard medical practice and the applications of research in rural medicine. **Robert A. McLaughlin** is Chair of Biophotonics at The University of Adelaide. His research focuses on the development of new optical imaging techniques to assess the microvasculature. In parallel, his team have also developed an imaging needle, which is a highly miniaturised fibre-optic imaging probe encased within a small stainless-steel hypodermic needle. These devices are capable of performing optical imaging deep within tissue and are finding applications in medicine and agricultural sciences. This current publication is the result of an on-going collaboration with Senior Author Professor Green to provide absolute quantification of blood flow in the microvasculature.
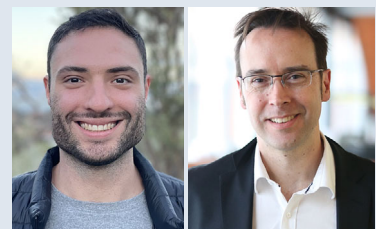
Introduction

Although heart failure (HF) symptoms are initiated by the impaired cardiac function which characterises the disease, chronic manifestations and functional limitations are often related to peripheral counter-regulatory adaptations (Clark et al., 1996). Peripheral vasoconstriction and elevated peripheral resistance are classic symptoms of HF (Maiorana et al., 2000) which, whilst maintaining blood pressure in the face of impaired ejection fraction, also act to reduce tissue blood flow and nutrition (Clark et al., 1996). Whilst previous studies have reported impaired conduit (Hambrecht et al., 2000) and resistance artery (Maiorana et al., 2000) function in HF, the structure and function of smaller microvessels have not previously been reported, due to an inability to directly image and quantify very small vessels *in vivo*.

Cutaneous microvessels play a crucial role in human thermoregulation (Johnson et al., 2014), responsible for enhancing heat loss in combination with sweat production and evaporation. Some previous evidence in humans indicates that HF patients exhibit difficulty thermoregulating (Green et al., 2006), with death rates spiking during heat waves (Cui & Sinoway 2014). Intrinsic cutaneous microvascular dysfunction may exacerbate thermoregulatory abnormalities in HF (Green et al., 2006). The current techniques used to assess vascular function, including ultrasound, angiograms, laser Doppler flowmetry and other optical techniques (Sen et al., 2016), are unable to directly image microvessels *in vivo*, and are therefore incapable of quantifying micro-vascular function at rest or in response to physiological stimulation.

Optical coherence tomography (OCT) is a high-resolution non-invasive imaging technique using low power near infrared light. OCT is commonly used in ophthalmology to image the retinal fundus (Girach & Sergott 2016), and we have recently optimised its use to image the skin microvasculature in humans (Argarini, McLaughlin, Naylor et al., 2020; Smith et al., 2019). Cutaneous OCT has shown the potential to provide quantitative metrics of average blood vessel diameter, blood density and blood flow (Smith et al., 2019) in vessels as small as $\sim$30 μm. In our recent studies, we have used OCT to accurately quantify cutaneous micro-vascular structure and function at rest and in response to physiological stimulation (e.g. responses to local heating) (Argarini, McLaughlin, Naylor et al., 2020; Smith et al., 2019). We have shown that OCT-derived measures are abnormal in diabetic subjects and that the degree of impairment corresponds with their disease severity (Argarini, McLaughlin, Joseph et al., 2020). In the current study we hypothesised that OCT-based metrics derived from the skin of HF subjects at rest and in response to heating would be impaired relative to a group of age-, body mass index (BMI)- and sex-matched controls.

Methods

Ethical approval

Ethics approval was granted by the Human Research Ethics Office at the University of Western Australia (ET000397). The study conformed to the standards outlined in the *Declaration of Helsinki* (except for registration in a database). All participants provided written informed consent.

Subject characteristics

Ten participants with end-stage HF (HF group: 8M, 2F, 57.5 ± 12.5 years, BMI: 27.9 ± 4.9 kg/m^2) were recruited from the Fiona Stanley Hospital Advanced Heart Failure Service in Perth, Western Australia. Diagnoses of HF were non-ischaemic dilated cardiomyopathy (6), rheumatic heart disease (1) and ischaemic cardiomyopathy (3). HF patients were matched on sex, age and BMI with 10 healthy controls (CON group: 8M, 2F, 58.1 ± 13.1 years, BMI: 26.8 ± 5.2 kg/m^2). Controls were recruited from the community and were screened to ensure none had pre-vious diagnoses of cardiovascular disease, diabetes, heart rhythm disturbances, vertigo, skin conditions or skin allergies.

Study design

Subjects attended a quiet and temperature-controlled room (23°C) in the Cardiovascular Research Laboratory, School of Human Sciences (Exercise and Sports Science) at The University of Western Australia. At the commencement of the testing session, participants' demographic data were documented, including age, sex, height and weight.

The participants lay supine for a period of at least 10 min with their arm comfortably supported by a foam pad, with the intention to minimise arm movement during the scanning session. After subjects were positioned, the OCT probe was placed on the area of interest on the ventral aspect of the subject's forearm, distal to the elbow, and angled to lie flush with the subject's skin. Immediately after OCT baseline images were obtained at a probe temperature of 33°C, the subject's skin was heated using a local heating disk (PF450, Perimed, Stockholm, Sweden) at a rate of 1°C per 10 s, from 33°C to 44°C. Upon reaching 44°C, the heater disk and skin temperature were maintained at 44°C for a further 30 min (Atkinson et al., 2018; Choi et al., 2014), whereupon the post-heating OCT scan was collected. We heated to 44°C to provide a stimulus that maximised the response, thereby providing

a surrogate measure of microvessel structure that removes the potentially differential influence of distinct functional mechanisms.

Experimental measures

Optical coherence tomography. OCT scans were acquired using a Telesto III imaging system (Thorlabs GmbH, Bergkirchen, Germany) and detachable imaging probe (LSM03, Thorlabs) with a central wavelength of 1300 nm, axial resolution of 5 μm in tissues (assuming refractive index of 1.43 for the skin) and lateral resolution of 13 μm. A three-dimensional (3D) printed spacer was used to house a heating element and ensure a standard distance between the imaging probe and skin surface whilst allowing for imaging to be performed through the central bore of the thermostatic probe holder (PF450, Perimed).

A small droplet of water was used as a refractive index-matching fluid between the skin and a transparent square microscope coverslip (8 × 8 mm) attached to the thermostatic probe holder. This provided a flat imaging surface and acted to reduce imaging artefacts due to differences in refractive index and local topography of the subject's skin.

Data were acquired over a field of view of 5 × 5 × 2.5 mm (length × width × depth) at a sampling rate of 1000 × 5000 × 1024 (x × y × z) pixels. OCT measurements (A-scans) were acquired at a rate of 146 kHz with a total scanning time of approximately 55 s. Speckle decorrelation analysis was performed on the A-scans as described elsewhere (Smith et al., 2019), producing 3D volume of displacement estimates.

Data analysis

Segmentation of OCT scans. The displacement estimates derived from the OCT scan indicate movement in the tissue during the scan acquisition. In non-vascular static tissue, the displacement values are negligible and indicative of noise in the measurement. In blood vessels, the estimated displacement is indicative of the blood flow. By identifying voxel regions of higher displacement, it is possible to automatically segment blood vessels from these scans, allowing automated quantification of the vasculature. Our experience has been that it is more robust to perform segmentation on a two-dimensional (2D) projection image, rather than the 3D volume. Conceptually, this is analogous to generating a maximum intensity projection image commonly used in MRI. From the OCT displacement volume data, we generate a 2D projection in the x–y plane (parallel to the skin surface). Three components are calculated at each x–y location, indicative of the amount of displacement due to blood flow, depth of the vessel, and a local estimate of the diameter of the vessel, respectively. Specifically, these three components are the maximum displacement value at (x,y); the depth of the maximum displacement value at (x,y); and the full width half-maximum range around the maximum displacement value (i.e. the z-range over which the displacement values are greater than half the maximum displacement). This generates a three-channel, 2D image of the vasculature which is used for segmentation. Areas of blood vessel and background were identified in the projection image by a modified ResNet neural network (He et al., 2016) which had been trained using the AdamW optimiser (Loshchilov & Hutter 2017) and on similar images not used in this study, which were manually segmented using ImageJ (Schneider et al., 2012).

Calculation of blood flow characteristics. The segmentations of the 2D projections into areas of blood vessel and background were then used to calculate values for the mean blood vessel density, mean blood vessel diameter, mean blood speed and mean blood flow rate (Argarini, McLaughlin, Naylor et al., 2020). All parameters were calculated according to the protocol outlined in previous studies (Smith et al., 2019). In summary, blood vessel density was calculated as the percentage of the pixels in the 2D projection image labelled as being blood vessel. To calculate the other parameters, the segmented 2D projection image was skeletonised to find the centreline of each vessel using standard imaging processing techniques of erosion and dilatation, and vessels were parameterised at each point along the centreline. Vessel diameter was estimated as the minimal distance across the vessel and blood speed estimated as the average taken over the points along this minimal distance path. The flow rate within a vessel was then calculated by approximating the vessel locally as a cylinder and quantifying flow rate as $F = s\pi r^2$, where s is the blood speed and r is the vessel radius (half the vessel diameter). At the completion of processing, values for diameter, speed and flow rate had been calculated at each point along the detected blood vessels, and mean values were computed over the entire field of view of the OCT scan. Changes in these parameters were analysed to identify any differences in blood vessels characteristics between HF patients and matched control subjects.

Statistical analysis

Sample size calculation was based on our previously published data which reported the difference in skin microvascular responses to local heating stimuli between diabetic subjects and controls (Argarini, McLaughlin, Joseph et al., 2020). Effect size and variance data derived from this study (Argarini, McLaughlin, Joseph et al., 2020) were entered into the formula of Hozo et al. (2005). Assuming a significance level of $\alpha = 0.05$ and $\beta = 0.8$,

the minimum number of subjects required to establish significance is seven per group (G*power, version 3.1.9.7) (Argarini, McLaughlin, Joseph et al., 2020).

The threshold for statistical significance was set to 0.05. Data were checked for normality using the Shapiro–Wilk test. Two-way repeated measures ANOVA was performed (SPSS 27.0, IBM Corp., Armonk, NY, USA) to calculate differences between groups, pre- and post-local heating, for OCT outcome measures. If a significant group × heating interaction was identified, simple main effects were calculated using one-way repeated measures ANOVAs or Student's paired *t*-test as appropriate. Changes from baseline were compared for HF *versus* controls using paired *t*-tests and all data are shown as means ± SD.

Results

Participant characteristics

There were no significant differences between HF and CON in age (HF *vs.* CON: 57.5 ± 12.5 *vs.* 58.1 ± 13.1 years,
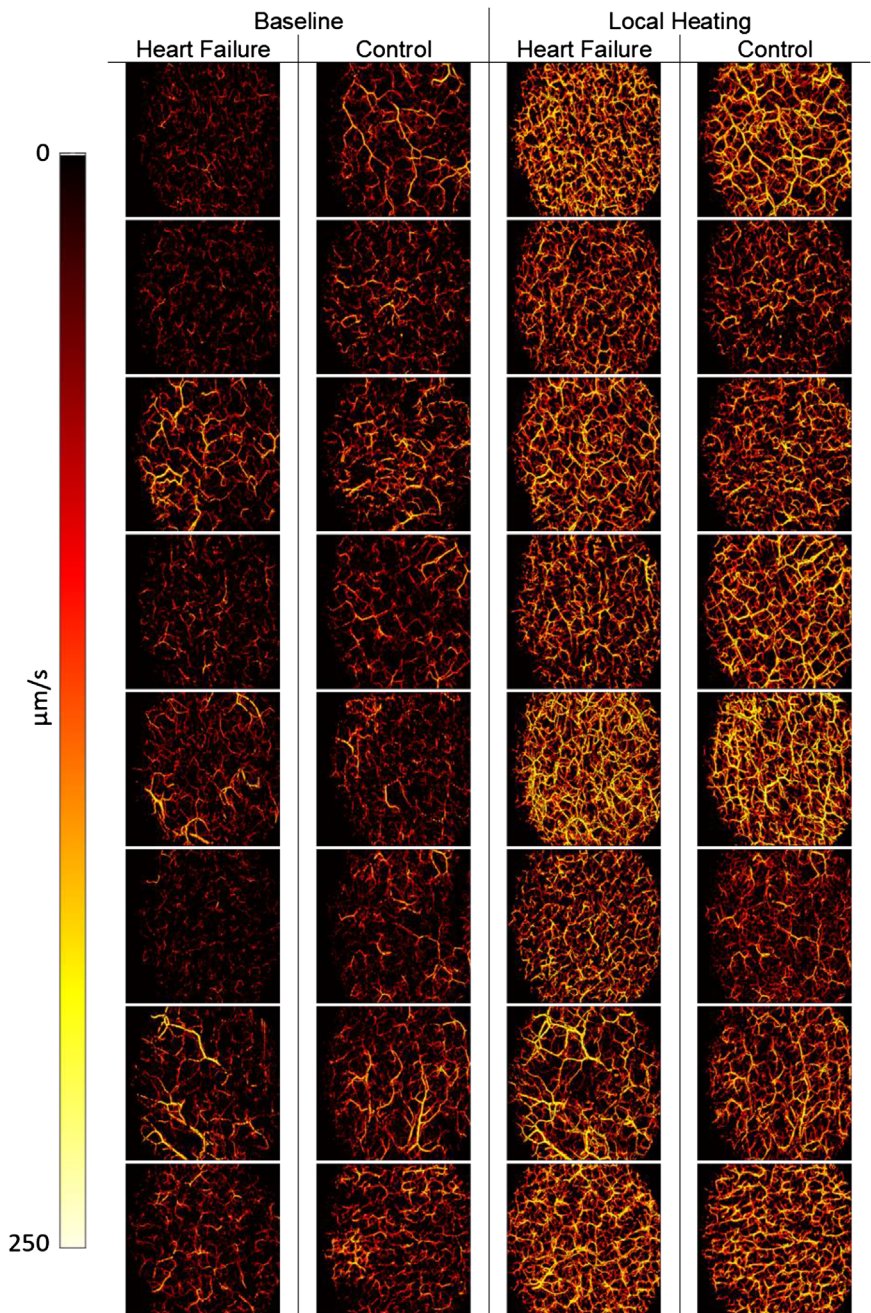

Figure 1. Qualitative comparison between OCT speed maps for a selection of HF patients and their matched controls at baseline and after local heating, showing microvasculature over a 5 × 5 mm field of view
Pixel intensity indicates flow speed, with dark red indicating slow flow and orange/yellow indicating faster flow. The baseline scans of those with HF were distinctly darker (indicating lower mean blood speed) than their matched controls. Once heated, the blood speed maps from both the HF patients and their matched controls appeared similar. [Colour figure can be viewed at wileyonlinelibrary.com]

Table 1. Cutaneous microvessel baseline and local heating responses using optical coherence tomography

Mean Estimate	HF (n = 10)	CON (n = 10)	P (t test)
Baseline (BL)			
Density (%)	20.3 ± 8.7	27.2 ± 8.0	0.004
Diameter (μm)	35.1 ± 6.0	40.4 ± 5.8	0.006
Speed (μm/s)	74.3 ± 11.0	81.3 ± 9.9	0.069
Flow (pl/s)	82.9 ± 41.1	110.8 ± 41.9	0.021
Local heating (LH)			
Density (%)	45.6 ± 7.9	44.2 ± 9.7	0.589
Diameter (μm)	51.4 ± 6.6	51.2 ± 7.7	0.926
Speed (μm/s)	134.9 ± 20.6	123.3 ± 28.1	0.228
Flow (pl/s)	282.4 ± 94.3	271.8 ± 129.1	0.774
Δ Heating (LH – BL)			
Density (%)	25.3 ± 4.8	17.0 ± 7.6	0.006
Diameter (μm)	16.3 ± 6.1	10.8 ± 6.1	0.110
Speed (μm/s)	60.6 ± 19.9	42.0 ± 27.2	0.055
Flow (pl/s)	199.5 ± 87.4	161.0 ± 115.4	0.337

Data are mean ± SD. Significance was determined with a two-tailed paired *t*-test. BL, baseline; LH, local heating; CON, Control; HF, heart failure.

$P = 0.434$) or BMI (27.9 ± 4.9 *vs.* 26.8 ± 5.2 kg/m^2, $P = 0.565$). Left ventricular ejection fraction in the HF subjects was $37 \pm 6.5\%$, New York Heart Association class II–III; systolic blood pressure was 101 ± 14 mmHg, diastolic blood pressure 56 ± 7 mmHg.

Typical images obtained from subjects at baseline and in response to heating are shown in Fig. 1. Baseline and local heating summary statistics for OCT-derived parameters (diameter, speed, flow rate and vessel density) for each group are presented in Table 1 and Fig. 2, with individual data also shown in Fig. 2.

Baseline OCT-derived parameters

At baseline, OCT-derived vessel density ($20.3 \pm 8.7\%$ *vs.* $27.2 \pm 8.0\%$, $P = 0.004$), vessel diameter (35.1 ± 6.0 *vs.* 40.4 ± 5.8 μm, $P = 0.006$) and flow rate (82.9 ± 41.1 *vs.* 110.8 ± 41.9 pl/s, $P = 0.021$) were lower in HF compared to CON (Table 1, Fig. 2). However, the OCT-derived parameter of blood speed (74.3 ± 11.0 *vs.* 81.3 ± 9.9 μm/s, $P = 0.069$) did not achieve statistical difference in HF compared to CON at baseline (Table 1, Fig. 2).

Effect of local heating on OCT-derived parameters

All OCT-derived peak heating parameters were similar in HF compared to CON (vessel density: $45.6 \pm 7.9\%$ *vs.* $44.2 \pm 9.7\%$, $P = 0.589$; diameter: 51.4 ± 6.6 *vs.* 51.2 ± 7.7 μm, $P = 0.926$; speed: 134.9 ± 20.6 *vs.* 123.3 ± 28.1 μm/s, $P = 0.228$; flow rate: 282.4 ± 94.3 *vs.* 271.8 ± 129.1 pl/s, $P = 0.774$; Table 1, Fig. 2).

Changes from baseline to peak heating

There were significant increases in OCT-derived diameter, vessel density, speed and flow rate following prolonged heating in both groups (all $P < 0.05$, Fig. 2 left panels). A significant group × heat interaction was found for the OCT-derived parameter of vessel density ($P = 0.006$, Fig. 2*A*). Correspondingly, the change with heating in OCT-derived vessel density was significantly higher in HF compared to CON (density/vessel recruitment: $25.3 \pm 4.8\%$ *vs.* $17.0 \pm 7.6\%$, $P = 0.006$, Table 1, Fig. 2*A*). The changes in OCT-derived vessel diameter, speed and flow rate were not different between HF and CON (diameter: 16.3 ± 6.1 *vs.* 10.8 ± 6.1 μm, $P = 0.110$; speed: 60.6 ± 19.9 *vs.* 42.0 ± 27.2 μm/s, $P = 0.055$ flow: 199.5 ± 87.4 *vs.* 161.0 ± 115.4 pl/s, $P = 0.337$; Table 1, Fig. 2*B–D*).

Discussion

We have established that OCT-based imaging is feasible and provides valuable quantitative insights into microvascular function and structure in HF. Our study suggests that HF subjects exhibit attenuated blood vessel density, diameter and flow rate under resting conditions compared to healthy matched controls, whereas measures collected in response to skin heating were not impaired in HF.

Microvascular abnormalities may logically present as impairment in function or as structural adaptation. In the present study we obtained data at rest and in response to a peak heating stimulus. This enabled us to distinguish the type of abnormality present in HF, since structural changes should be persistently apparent. Our observation
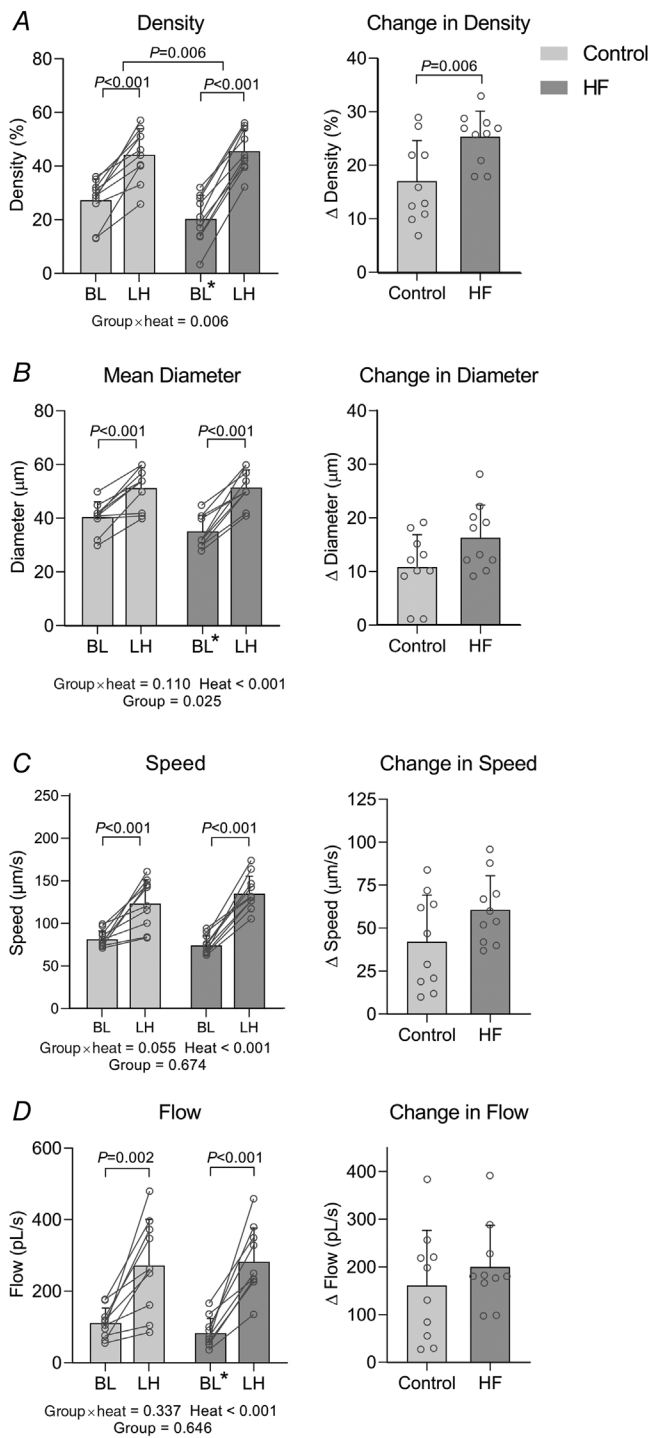
Figure 2. Mean blood vessel density (%) (*A*), diameter (μm) (*B*), blood speed (μm/s) (*C*), and blood flow (pl/s) (*D*) for heart failure patients (dark grey, *n* = 10) and matched controls (light grey, *n* = 10) at baseline (BL) and after local heating (LH)
Data are means ± SD, individual data overlaid, repeated measures ANOVA (left panels) and paired *t*-tests (right panels). LH responses relative to their baseline are shown on right hand panels. *Difference from control group at $P < 0.05$.

that differences in OCT-derived density, diameter and flow rate were apparent at rest, but not in response to a peak heating stimulus, implies that a functional microvascular impairment is present in HF. This may relate to the mechanisms responsible for control of microvascular tone. It is well established that the sympathetic nervous system is more highly activated in HF, as a counter-regulatory reflex to sustain blood pressure in the face of impaired cardiac function (Bauersachs et al., 2017). Enhanced sympathetic tone is consistent with our findings regarding attenuated basal microvascular parameters, but we cannot rule out other mechanisms, including dysfunctional local paracrine bioavailability of vasoactive hormones (e.g. nitric oxide, prostacyclin, endothelium-derived hyperpolarizing factor, histamine, etc.) (Johnson et al., 2014; Low et al., 2020; Wong & Hollowed 2017).

Previous studies using more indirect techniques have estimated microvascular outcomes in HF subjects. For example, Wroblewski et al. (1995) suggested that the cause of microvascular dysfunction in HF was structural in nature, using indirect radiation-based measurements to estimate blood flow and vascular resistance. They concluded that the distensibility (stiffness) of blood vessels was attenuated in HF patients, suggesting a structural change in the microvasculature. In contrast, studies utilising laser Doppler flowmetry have indicated that HF subjects have impaired responses to heating, and that this may relate to abnormal NO-mediated vasodilator function (Green et al., 2006). As laser Doppler flowmetry does not provide images, measurements calculated using this technique cannot assess vessel diameter or volumetric flow. This contrasts with OCT, which allows for the visualisation and quantification of blood movement, with the added benefit of blood flow being directly calculated.

In a recent study we established that patients with diabetes had abnormal OCT-derived cutaneous microvascular function compared to healthy matched controls, and that the microvasculature of diabetics with foot ulceration was more dysfunctional than in those without ulcers (Argarini, McLaughlin, Joseph et al., 2020). This promising finding suggests that OCT may provide insights related to microvascular disease severity or progression. Of interest, diabetic subjects had exaggerated resting OCT-derived density, diameter, blood speed and flow rate measures compared to the controls, which contrasts with our findings in HF. This is reassuring, since the pathophysiology of microvascular disease likely differs between HF and diabetic subjects, whereby the former is characterised by elevated peripheral resistance and impaired cardiac function, whilst the latter exhibit localised tissue inflammatory cascades. The impact of other disease states, or indeed ageing *per se* might be the focus of future studies involving cutaneous OCT.

Whilst cutaneous measures may provide insight into systemic microvascular health (Holowatz et al., 2008) status, skin vascular function is also directly relevant to thermoregulatory function in humans (Kenney et al., 2014; Simmons et al., 2011). It is well established that heat waves are associated with excess mortality (Kenney et al., 2014), particularly in subjects with cardiovascular disease and, specifically, HF (Cui & Sinoway 2014). Whilst we used local heating in the current study, future experiments may utilise OCT to provide important novel information regarding the function of skin microvessels during core and/or environmental heating. OCT may also provide a powerful platform to assess adaptations that occur with heat acclimation and exercise training, as previous studies have suggested some beneficial effects of these interventions on cardiovascular health (Kihara et al., 2002; Kunutsor et al., 2018; Laukkanen et al., 2015).

OCT, which is non-invasive and does not use ionising radiation, can be used at the patient's bedside to assess microvascular status and therefore represents a potentially useful technological advance, particularly if the easily obtained cutaneous measures are indicative of systemic microvascular status. However, this study has several limitations, including the small sample size, although an *a priori* test based on previous studies indicated that our OCT approach is sufficiently sensitive to provide adequate power to detect the differences we observed between HF and control subjects. Future larger studies, perhaps comparing subjects of differing aetiology, are nonetheless warranted. Future studies should also focus on assessing whether OCT measures, and changes in OCT with treatment, predict clinical outcomes in HF. Finally, OCT is not currently capable of assessing changes in blood flow or diameter with high temporal resolution, and future technological development should address this limitation.

References

Argarini, R., McLaughlin, R. A., Joseph, S. Z., Naylor, L. H., Carter, H. H., Yeap, B. B., Jansen, S. J., & Green, D. J. (2020). Optical coherence tomography: a novel imaging approach to visualize and quantify cutaneous microvascular structure and function in patients with diabetes. *BMJ Open Diabetes Research and Care*, **8**(1), e001479.

Argarini, R., McLaughlin, R. A., Naylor, L. H., Carter, H. H., & Green, D. J. (2020). Assessment of the human cutaneous microvasculature using optical coherence tomography: Proving Harvey's proof. *Microcirculation*, **27**(2), e12594.

Atkinson, C. L., Carter, H. H., Thijssen, D. H. J., Birk, G. K., Cable, N. T., Low, D. A., Kerstens, F., Meeuwis, I., Dawson, E. A., & Green, D. J. (2018). Localised cutaneous microvascular adaptation to exercise training in humans. *European Journal of Applied Physiology*, **118**(4), 837–845.

Bauersachs, J., Butler, J., & Sandner, P. (2017). *Heart Failure*. Springer International Publishing, Champaign.

Choi, P. J., Brunt, V. E., Fujii, N., & Minson, C. T. (2014). New approach to measure cutaneous microvascular function: An improved test of NO-mediated vasodilation by thermal hyperemia. *Journal of Applied Physiology*, **117**(3), 277–283.

Clark, A. L., Poole-Wilson, P. A., & Coats, A. J. (1996). Exercise limitation in chronic heart failure: Central role of the periphery. *Journal of the American College of Cardiology*, **28**(5), 1092–1102.

Cui, J., & Sinoway, L. I. (2014). Cardiovascular responses to heat stress in chronic heart failure. *Current Heart Failure Reports*, **11**(2), 139–145.

Girach, A., & Sergott, R. C. (2016). *Optical coherence tomography*. Springer International Publishing, Champaign.

Green, D. J., Maiorana, A. J., Siong, J. H., Burke, V., Erickson, M., Minson, C. T., Bilsborough, W., & O'Driscoll, G. (2006). Impaired skin blood flow response to environmental heating in chronic heart failure. *European Heart Journal*, **27**(3), 338–343.

Hambrecht, R., Hilbrich, L., Erbs, S., Gielen, S., Fiehn, E., Schoene, N., & Schuler, G. (2000). Correction of endothelial dysfunction in chronic heart failure: Additional effects of exercise training and oral L-arginine supplementation. *Journal of the American College of Cardiology*, **35**(3), 706–713.

He, K., Zhang, X., Ren, S., & Sun, J. (2016). Deep residual learning for image recognition. In *Proceedings of the IEEE conference on computer vision and pattern recognition*, pp. 770–778.

Holowatz, L. A., Thompson-Torgerson, C. S., & Kenney, W. L. (2008). The human cutaneous circulation as a model of generalized microvascular function. *Journal of Applied Physiology*, **105**(1), 370–372.

Hozo, S. P., Djulbegovic, B., & Hozo, I. (2005). Estimating the mean and variance from the median, range, and the size of a sample. *BMC Medical Research Methodology*, **5**(1), 13.

Johnson, J. M., Minson, C. T., & Kellogg, D. L., Jr(2014). Cutaneous vasodilator and vasoconstrictor mechanisms in temperature regulation. *Comprehensive Physiology*, **4**, 33–89.

Kenney, W. L., Craighead, D. H., & Alexander, L. M. (2014). Heat waves, aging, and human cardiovascular health. *Medicine and Science in Sports and Exercise*, **46**(10), 1891–1899.

Kihara, T, Biro, S., Imamura, M., Yoshifuku, S., Takasaki, K., Ikeda, Y., Otuji, Y., Minagoe, S., Toyama, Y., & Tei, C. (2002). Repeated sauna treatment improves vascular endothelial and cardiac function in patients with chronic heart failure. *Journal of the American College of Cardiology*, **39**(5), 754–759.

Kunutsor, S. K., Khan, H., Laukkanen, T., & Laukkanen, J. A. (2018). Joint associations of sauna bathing and cardiorespiratory fitness on cardiovascular and all-cause mortality risk: A long-term prospective cohort study. *Annals of Medicine*, **50**(2), 139–146.

Laukkanen, T., Khan, H., Zaccardi, F., & Laukkanen, J. A. (2015). Association between sauna bathing and fatal cardiovascular and all-cause mortality events. *JAMA Internal Medicine*, **175**(4), 542–548.

Loshchilov, I., & Hutter, F. (2017). Decoupled weight decay regularization. *arXiv preprint arXiv:171105101*.

Low, D. A., Jones, H., Cable, N. T., Alexander, L. M., & Kenney, W. L. (2020). Historical reviews of the assessment of human cardiovascular function: Interrogation and understanding of the control of skin blood flow. *European Journal of Applied Physiology*, **120**(1), 1–16.

Maiorana, A., O'Driscoll, G., Dembo, L., Cheetham, C., Goodman, C., Taylor, R., & Green, D. (2000). Effect of aerobic and resistance exercise training on vascular function in heart failure. *American Journal of Physiology. Heart and Circulatory Physiology*, **279**(4), H1999–H2005.

Schneider, C. A., Rasband, W. S., & Eliceiri, K. W. (2012). NIH Image to ImageJ: 25 years of image analysis. *Nature Methods*, **9**(7), 671–675.

Sen, C. K., Ghatak, S., Gnyawali, S. C., Roy, S., & Gordillo, G. M. (2016). Cutaneous imaging technologies in acute burn and chronic wound care. *Plastic and Reconstructive Surgery*, **138**, 119S–128S.

Simmons, G. H., Wong, B. J., Holowatz, L. A., & Kenney, W. L. (2011). Changes in the control of skin blood flow with exercise training: Where do cutaneous vascular adaptations fit in? *Experimental Physiology*, **96**(9), 822–828.

Smith, K. J., Argarini, R., Carter, H. H., Quirk, B. C., Haynes, A., Naylor, L. H., McKirdy, H., Kirk, R. W., McLaughlin, R. A., & Green, D. J. (2019). Novel noninvasive assessment of microvascular structure and function in humans. *Medicine and Science in Sports and Exercise*, **51**(7), 1558–1565.

Wong, B. J., & Hollowed, C. G. (2017). Current concepts of active vasodilation in human skin. *Temperature*, **4**(1), 41–59.

Wroblewski, H., Nørgaard, T., Haunsø, S., & Kastrup, J. (1995). Microvascular distensibility in two different vascular beds in idiopathic dilated cardiomyopathy. *American Journal of Physiology*, **269**, H1973-1980.

Additional information

Data availability statement

All data are included as individual data in the figures contained in this manuscript.

Competing interests

R. A. McLaughlin is a co-founder and Director of Miniprobes Pty Ltd, a company that develops novel optical imaging systems. Miniprobes Pty Ltd did not contribute to this study.

Author contributions

D.F.G.S., R.A.M., R.A., L.H.N. and D.J.G. conceived and designed the experiments; D.F.G.S., M.S.T. and R.A.M. conceived and implemented the image analysis algorithms; D.F.G.S., R.A., H.H.C. and L.M.B. recruited participants and collected data; D.F.G.S. and R.A.M. analysed data; and D.F.G.S., R.A.M. and D.J.G. wrote the manuscript with input from all authors. All authors approved the final version of the manuscript and agree to be accountable for all aspects of the work, in ensuring that questions related to the accuracy or integrity of any part of the work are appropriately investigated and resolved. All persons designated as authors qualify for authorship and all those who qualify for authorship are listed.

Funding

Acknowledgements

Keywords

heart failure, microvessels, optical imaging

Supporting information

Additional supporting information can be found online in the Supporting Information section at the end of the HTML view of the article. Supporting information files available:

Statistical Summary Document
Peer Review History